Peer-reviewed version available at *Appl. Sci.* **2018**, *8*, 2046; doi:10.3390/app8112046

Communication

Photo-Assisted Hydrogen Evolution with Reduced Graphene Oxide Catalyst on Silicon Nanowire Photocathode

Yelyn Sim[1,‡], Jude John[1,‡], Joonhee Moon[2,*], and Uk Sim[1,*]

1 Department of Materials Science & Engineering, Chonnam National University, Gwangju 61186, Republic of Korea
2 Advanced Nano-Surface Research Group, Korea Basic Science Institute, Daejeon 34133, Republic of Korea
* Correspondence: junnymoon@kbsi.re.kr, usim@jnu.ac.kr ; Tel.: +82-42-865-3652, +82-62-530-1718

Abstract: Silicon-based photoelectrochemical (PEC) conversion system has recently gained attention with its ability to provide cost-efficient and superior photoresponsive behavior in regard to other various semiconductor photoelectrodes. Carbon-based co-catalysts have always shared the spotlight for being rendered as alternative metal-free electrocatalysts intended for hydrogen evolution reaction (HER). In particular, a representative carbon-derived material, reduced graphene oxide (rGO) has attracted much attention as a non-metal catalyst for efficient and durable HER. Herein, we have deposited rGO on silicon nanowire (SiNW) structure which shows the highest reduction in the overpotential for HER up to date. This could be attributed to the synergistic effects of rGO and SiNW with unique anisotropic morphology, facile tuning capabilities, and scalable fabrication methods. Combined with nanostructured photocathode, rGO deposited SiNW showed better applied bias photon to current conversion efficiency of 3.16%, which is 158 times higher than that of bare planar Si system. In regard to this development we believe that rGO-SiNW photoelectrodes would pave the way for state-of-the-art highly efficient non-metal catalysts for energy conversion technologies.

Keywords: silicon nanowire (SiNW), hydrogen evolution reaction (HER), reduced graphene oxide

1. Introduction

Precipitous rise in energy consumption worldwide has shifted the focus towards finding an environmentally benign energy source.[1] Exploring alternatives towards sustainable energy production is on the rise wherein photoelectrochemical splitting of water tops the lists of being clean source of energy.[2-3] Hydrogen production through water splitting is crucial for a clean source of energy since water splitting has zero contribution for CO_2 generation.[4] Being an earth abundant material, silicon (Si) has gained massive attention in the area of photo assisted light harvesting as Si possesses a narrow band gap allowing it to absorb solar radiation ranging from the ultraviolet region to visible light region.[5] Concurrently, one-dimensional nanostructures demonstrate promising applications in the area of photovoltaics owing to their remarkable enhancement in optical absorption in comparison with the bulk and zero dimensional materials. [6 7 8]

However, Si electrode often is encountered with a tremendous challenge of the high overpotential that required in generating hydrogen. Thus, developing significantly highly efficient electrode which can overcome the drawbacks posed by Si is crucial. Various approaches have been explored to improve the photoelectrochemical response of one-dimensional Si nanostructures, especially Si nanowire (SiNW) structure including surface modifications accompanied with cost considerations and natural abundance of the electrocatalyst are taken into consideration. Si based photoelectrodes can be

Scheme 1. Illustration of the structure of reduced graphene oxide (rGO) on Silicon nanowire photocathode.

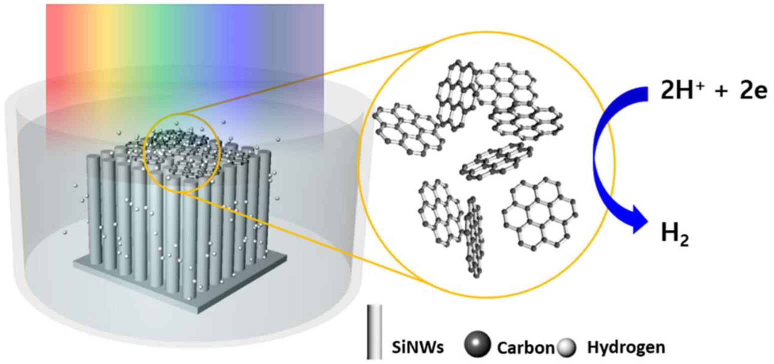

employed to be used as both photocathode and photoanode for water splitting reactions especially owing to its narrow band structure.[9-11] A fundamental problem observed with a low-band gap Si as a photocathode for H_2 generation is the difference between the Si valence band edge and the H^+/H_2 redox level is quite narrow, which limits the generation of a photovoltage.[12]

As an emerging class of two-dimensional material, graphene has achieved much attention in numerous applications owing to its stability, higher surface area, better optical transparency and a high carrier mobility. Reduced graphene oxide (rGO) a promising candidate of carbon-based materials is often employed in this regard because of its exceptional photoelectrochemical water splitting capability and also for its fast-interfacial charge transfer between the electrode surface and the electrolyte.[13-14] rGO was chosen as the co-catalyst in this current work for photoelectrochemical water splitting reactions.

Herein, we report a simple but convenient fabrication of rGO-SiNW composite to amplify the photoelectrochemical response towards hydrogen evolution reaction (HER) as shown in Scheme 1. In order to minimize the recombination rate on the electrode surface and thus increasing the efficiency, we adapted the SiNW structure which contributes to higher light absorption and charge carrier collection.[15-16] The photoelectrochemical performance could be further tuned by transforming the plane surface of Si electrode to that of a wire. Moreover, the high surface to volume ratio accompanied with its unique optoelectronics properties could be advantageous for various applications. This distinctive surface property also allows us to reduce light being reflected of the surface of a planar Si electrode. Yet another noteworthy factor is the length of Si nanowire which also contributes in enhancing the efficiency.[17-19] As a result, in our experiment we used a 22 μm long SiNW. We also conducted studies for optimization of photoelectrode through surface treatment for a better PEC response towards HER along the interface between rGO and SiNW substrate. The cyclic voltammetry studies and the transient photoresponse for the Si electrode yielded a smallest value and displayed a strong band bending for enhanced HER.[16] Considering the excellent optical absorption capability of the rGO/SiNW composite and the innumerous possibilities of chemically modifying graphene and fabrication method followed here, we believe that the step in the progressive direction in discovering and employing new materials and synthesis approaches towards high efficient photoelectrochemical hydrogen production.

2. Materials and Methods

Synthesis of graphene oxide. Graphene oxide was synthesized by Hummer's method.[20] First, the mixture of graphite powder (5 g) and $NaNO_3$ (3.8 g) was put into a flask, which was cooled in an ice bath. An aqueous H_2SO_4 (170 ml) was added into the flask with magnetic stirring. $KMnO_4$ (22.5 g) powder acting as an oxidation agent was gradually put into the flask over 1 h and it was maintained for 2 h with continuous stirring. Then, the ice bath was removed and the flask filled with the mixture

Peer-reviewed version available at Appl. Sci. 2018, 8, 2046; doi:10.3390/app8112046

was vigorously stirred. After 5 days, the color of the graphite was changed to brown-color viscous slurry. An aqueous de-ionized water (300 ml) was added into the flask over 1 h with stirring system. Additionally, 30 wt% H_2O_2 (5 ml) was added into the mixture with continuously stirring and it was maintained for 2 days. Finally, the mixture was rinsed with de-ionized water (6000 ml) using a centrifuge system and dialyzed for 7 days. Graphene oxide powder could be obtained by rotary vacuum evaporator system. Graphene oxide powder was placed in the center of the petri dish with tissue wetted by hydrazine (2 ml), and it is heated up to 80℃ for 20 min. Then, brown color GO was changed to reduced graphene oxide (rGO).

Fabrication of silicon nanowire structure. Boron-doped p-type single crystalline Si wafer was purchased from Namkang (500 μm thickness, 4 inch diameter, 10–15 Ω·cm resistivity, and (100) orientation). $AgNO_3$ powder (99.5%) and HF (48–51 wt%) were purchased from Sigma Aldrich and concentrated nitric acid solution (70 wt%) purchased from Daejung Chemical. Si wafers were cut to dimensions of 8 x 8 mm^2 and then each of the Si wafers were cleaned with acetone, 2 propanol and deionized water each for 10 min respectively using bath sonication. 20mL aqueous solution of $AgNO_3$ (0.679 g, 0.02 M) and HF (5 M) were used to etch and form nanowire structure on the planar Si surface. Finally, Ag residue on the nanostructured Si surface was removed completely by treating with 70% nitric acid solution for two hours.

Preparation of Si photocathode. For the ohmic contacts between the backside of silicon wafer and the copper wire, Gallium-Indium eutectic alloy (Kojundo Chemical Inc.) was used along with silver paste. To protect and insulate the backside of silicon wafer, epoxy (Loctite Hysol 9460) was used except for the illumination area (0.25 cm^2) of the Si front side.

Electrochemical measurements. Electrochemical measurements were performed using the three-electrode cell (CHI 7008E, CH Instruments, Inc., customized). The Pt wire was served as the counter electrode and Ag/AgCl/3M NaCl electrode was used as the reference electrode. The reference electrode was carefully calibrated with respect to Reversible Hydrogen Electrode (RHE) in an aqueous 1 M perchloric acid solution with high purity hydrogen saturation at 25℃. The RHE was calibrated to -0.200 V vs. the reference electrode. 100W Xenon lamp was used as the light source with a light intensity of 100 mW/cm^2 (Air Mass 1.5 Global condition glass filter) was employed for solar irradiation. Compact Rotating Disk Electrode (RDE, Pine Inc.) measurement was performed with glassy carbon (GC) tip (dia. 5mm). RDE measurement was done at a rotating speed of 1,000 rpm with a scan rate of 10 mV/sec.

3. Results and Discussion

Silicon nanowire (SiNW) structure was fabricated by metal-catalyzed electroless chemical etching method. The length of nanowire was controlled by controlling the etching time. Figure 1 shows the Scanning electron microscope (SEM) images of SiNW photoelectrode deposited with reduced graphene

doi:10.20944/preprints201809.0297.v1

Peer-reviewed version available at *Appl. Sci.* **2018**, *8*, 2046; doi:10.3390/app8112046

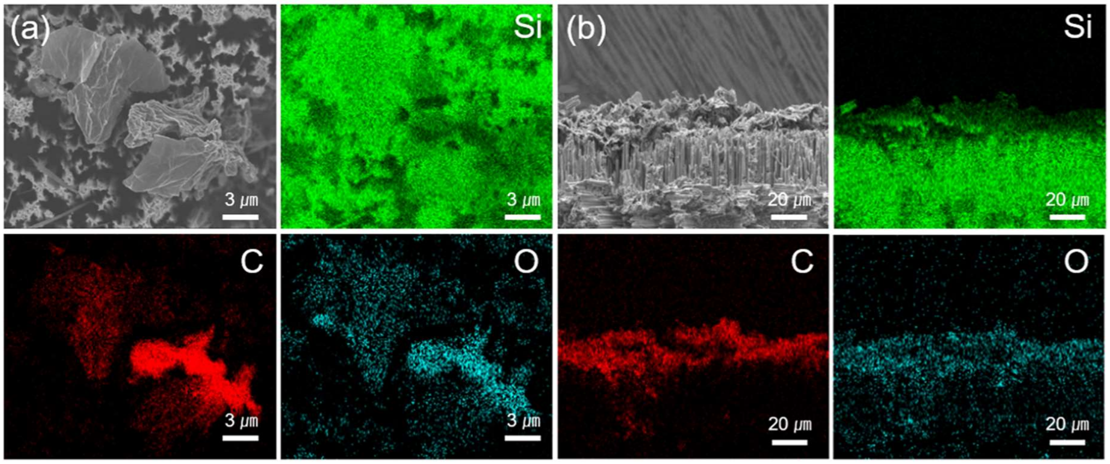

Figure 1. (a) Plan-view SEM image and EDS elemental images of Si, C, and O (b) Cross sectional SEM image and EDS elemental images of Si, C, and O.

oxide (rGO) and energy-dispersive X-ray spectroscopy (EDS) which shows each element of photoelectrode. We observed the elements of Silicon, Oxygen, and Carbon which are composed of rGO, of which are grown homogenously on SiNW photoelectrode through the EDS image. Cross sectional SEM image also showed uniform coating of rGO onto the SiNW with the average length of 22μm.

To provide more insights into the photocathodic efficiency of the SiNW photoelectrode, the inherent current density was measured in the potential window range of from 0.4 V to -0.7 V vs. RHE using a three-electrode cell. The light intensity in our setup was 100mW/cm^2 which was passed through an Air Mass 1.5 Global filter, 300 Xe lamp was used in aqueous 1 M perchloric ($HClO_4$) at acidic condition (pH=0). Figure 2 shows the linear sweep voltammogram graph under light illumination showing current density according to the specific applied potential. At first, the reductive current density started to increase from specific point as the applied potential increased negatively. The current density saturates at enough higher applied potential, which is often described as limiting current density or saturation current density. The onset potential is defined as the current density is reached at -1 mA/cm^2 which also indicates that the starting point of current density at the specific potential determines the extent of the requirement for power to generate hydrogen. The onset potential of SiNW electrode under illumination is 0.179 V vs. RHE, while bare planar Si electrode only shows -0.106 V vs. RHE. (Figure 2 and Table 1). Saturation current density also increased when the surface nanostructuring was implemented. The saturation current density of SiNW showed 38.2 mA/cm^2, which is approximately 1.2 times higher than that of bare planar Si (32.8 mA/cm^2). To calculate the solar-to-hydrogen conversion efficiency (STH), the concept of applied bias photon-to-current efficiency (ABPE, or half STH) was introduced according to the following equation,

$$\text{ABPE} = [j_{ph}(\text{mA/cm}^2) \times (V_{redox}-V_b)(\text{V})/P_{in}(\text{mW/cm}^2)]_{\text{AM1.5G}} \times 100(\%)$$

where j_{ph} is the photocurrent density obtained under the applied potential V_b, V_{redox} is the redox potential needed for hydrogen production (0 V vs. RHE), V_{bias} is the applied external bias potential that is often necessary to achieve reasonable photocurrents, and P_{light} is the intensity of the incident incident light under AM 1.5 G conditions (100 mW/cm^2). Compared to bare planar Si electrode, SINW electrode system exhibited 46 times higher ABPE (Table 1). The enhanced current density including limiting current density can be mainly explained by increased surface area by surface nanostructuring. The nanowire structure in turn increases the current density of Si photocathode whereby increasing the number of effective reaction sites on the illuminated surface. Moreover, reduced reflection also increases the possibility of enhanced incident light collection. It is also known that bare planar Si reflects

Peer-reviewed version available at Appl. Sci. 2018, 8, 2046; doi:10.3390/app8112046

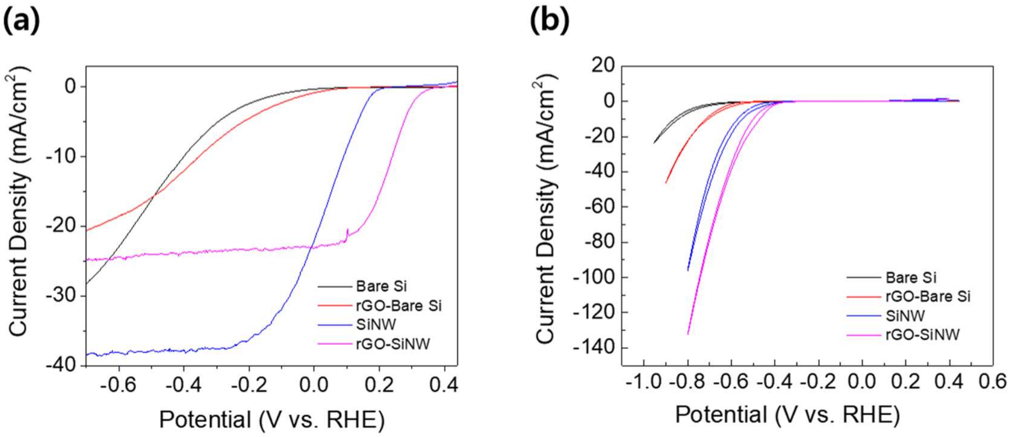

Figure 2. Cyclic voltammograms of rGO on silicon photocathodes. (a) Photoresponse current density-potential curves for bare planar Si and Si nanowire with/without deposition of rGO. (b) Polarization curves of rGO on Si electrodes under dark condition.

about 25% of the incident light,[21] but nanostructured surface decreases photon absorption significantly due to the low reflectance. For this reason, SiNW structure electrode exhibits higher light trapping effect which shows enhanced photon-to-current conversion efficiency than that of bare planar Si electrode. Moreover, orthogonalization reduces the recombination rate between electron and hole pair, which is generated in the photoelectrode. The nanowire structure has a relatively shorter horizontal length compared to the length of vertical direction, this structure allows for the generated minority carrier (electrons) to move to faster in lateral side of electrode and to meet the proton in the electrolyte to produce hydrogen. Consequently, the potential for the water spitting reaction approaches theoretical value with a decreased kinetic barrier for the hydrogen generation, resulting in the increased onset potential as shown in Figure 2a. In the dark condition, the onset potential for the bare planar Si electrode shows -0.656 V vs. RHE and SiNW electrode exhibits -0.448 V vs. RHE. Interesting point is that the degree of onset potential shift from bare Si to SiNW in both light and dark conditions shows almost same (about 0.2 V vs. RHE). From the results, the photovoltage of bare Si and SiNW electrodes are 0.55 V vs. RHE and 0.62 V vs. RHE, indicative that with the nanowire structure an increased photovoltage is observed under both light and dark condition and a decreases in the kinetic barrier for the hydrogen production.

rGO catalyst further enhances photoelectrochemical property of Si photocathode. Figure 2 shows photoelectron-catalytic performance of rGO on SiNW toward HER. rGO deposited on SiNW photocathode showcased an onset potential of 0.326 V vs. RHE which is much larger than bare SiNW photoelectrode (0.147 V vs. RHE) . In the dark condition, the difference in the overpotential between rGO-SiNW and SiNW was 66 mV. The saturation current density of rGO-SiNW somewhat decreased (25mA/cm^2) compared to the bare SiNW, which is attributed to the light hindrance by opaque rGO. The reduced reflection is also identified with the optical spectrum measurement as shown in Figure 3, eventually, the overall solar-to-current conversion efficiency increased by the introduction of the rGO co-catalyst. rGO-deposited SiNW showed better photon to current conversion efficiency of 3.16%, which is 158 times higher than that of bare planar Si system (Table 1). As a result, rGO works as an effective HER co-catalyst on the Si electrode owing to the synergistic effects between rGO and SiNW is solely responsible for the improved photocatalytic performance.

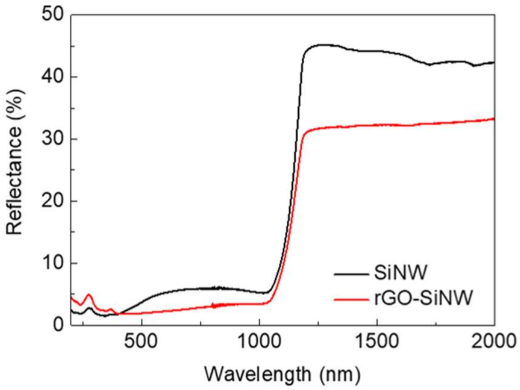

Figure 3. Optical spectrum of the Si surface. Reflectance of bare SiNW and rGO-SiNW composite.

Table 1. Summary of the experimental data of Si and Glassy Carbon (GC) electrode

	Electrode	**Onset potential [E(V) at -1mA/cm^2]**	**E(V) at -5mA/cm^2**	**E(V) at -10mA/cm^2**	**Current density at reversible potential vs. RHE [mA/cm^2 at 0V vs. RHE]**	**ABPE(%)***
Under illumination (p type Si)	Planar Si	-0.106	-0.295	-0.401	-0.293	0.02
	Si NW	0.179	0.133	0.090	-22.00	0.91
	rGO-planar Si	-0.018	-0.217	-0.354	-0.619	0.03
	rGO-SiNW	0.326	0.275	0.239	-23.152	3.16
Under dark condition (n^+type Si)	Planar Si	-0.656	-0.771	-0.843		
	Si NW	-0.448	-0.527	-0.571		
	rGO-planar Si	-0.579	-0.663	-10.04		
	rGO-SiNW	-0.382	-0.434	-0.47		
Photovoltage	Planar Si	0.550				
	Si NW	0.627				
	rGO-planar Si	0.561				
	rGO-SiNW	0.708				
RDE analysis	Bare GC	-0.397	-0.778	-		
	rGO-GC	-0.250	-0.345	-0.389		

* ABPE : applied bias photon-to-current efficiency

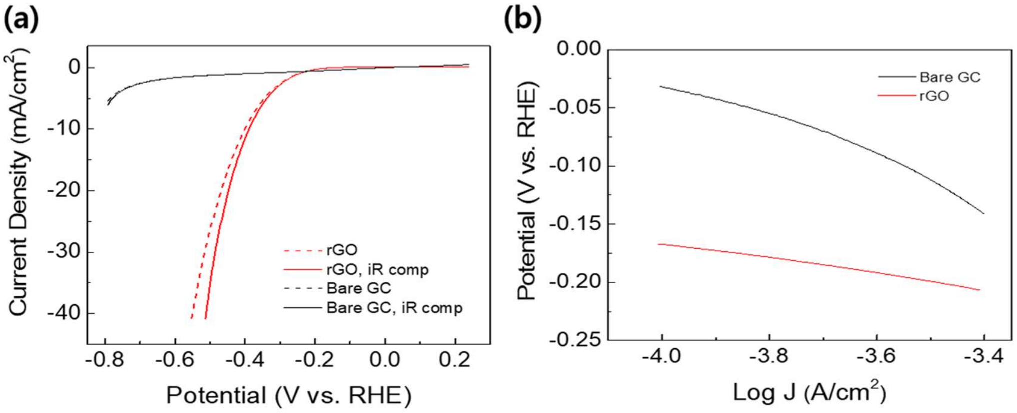

Figure 4. Electrochemical activity of a bare glassy carbon (CG) electrodes in a rotating disk electrode system. (a) Cyclic voltammograms of bare GC and rGO on GC electrodes. CV data obtained compensating for ohmic drop (iR) losses are also plotted (dash curves). (b) Tafel plots derived from CV data in (a).

In order to shed more light into the electrocatalytic activity of the rGO catalyst, capacitance studies were performed using a rotating disk electrode (RDE) system (Figure 4). The catalyst ink comprising of rGO was drop-casted on to the glassy carbon (GC) tip. The significant rise in the current density at the same potential for rGO on GC compared to that of the bare GC can be explained by the electrochemically active catalyst (rGO) which can further improve the water splitting efficiency towards HER. When considering the resisting arising between electrolyte and the electrode interface, it would be necessary to consider iR compensation. After iR compensation, the onset potential of rGO decreased significantly. To study the catalytic effects of rGO, Tafel plots for rGO/SiNW were performed (Figure 4b). Tafel slope provides the appropriate pathway suitable for HER:[22]

$H_3O^+ + e^- \rightarrow H_{ads} + H_2O$ Volmer reaction (1)
$H_{ads} + H_3O^+ \rightarrow H_2 + H_2O$ Heyrovsky reaction (2)
$H_{ads} + H_{ads} \rightarrow H_2$ Tafel plot (3)

where H_{ads} is absorbed H, (1) is a discharge step, (2) desorption of H-atom, and (3) is the recombination. The measured Tafel slope was found to be 30 mV per decade. Nevertheless, in the case of electrochemical desorption step (the Heyrovsky reaction) can be regarded as the rate-determining step here, and a Tafel slope of 40-118 mV per decade is measured which is dependent of the value observed for θ_H (0 to 1). The Tafel slope of 45 mV per decade in our work indicates that the kinetic of the HER on the rGO catalyst was found to follow the Heyrovsky reaction

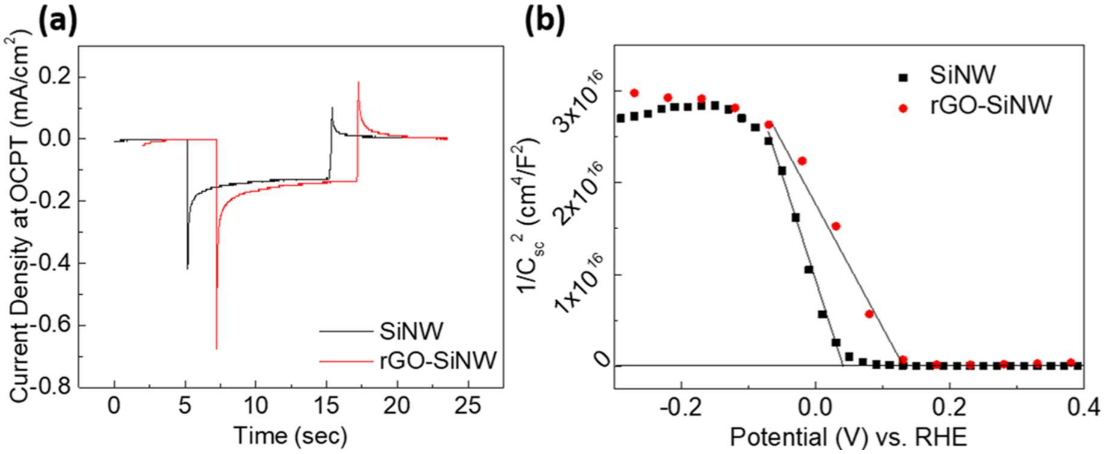

Figure 5. Electrochemical activity of SiNW and rGO-SiNW. (a) The transient curve of the photocurrent from SiNW and rGO-SiNW when the light was turned on and off near at open circuit potential region (OCPT). (b) Mott-Schottky plot from capacitance measurement

Comprehensive electrochemical measurements on rGO-SiNW system also shows the efficient roles of the rGO catalyst as shown in Figure 5. The transient photoelectrochemical behavior of the rGO-SiNW is also dependent on limiting the illumination time range. Figure 5a shows the transient photoresponse of the rGO-SiNW and bare SiNW electrode. With a 10 sec interval the light was turned on and off, while the potential was maintained near at open circuit potential (OCPT) vs RHE. As shown in Figure 5a, the initial rise in the photocurrent density (J_{in}) was -0.70 mA/cm^2 for rGO-SiNW and -0.45 mA/cm^2 for SiNW, respectively was caused by the sudden turning on of light source. After taking the culmination, the current density saturated at certain point called the saturated photocurrent density (J_{st}). Under illumination, the value of J_{st}, -0.19 mA/cm^2 is for the rGO-SiNW, which is higher than that of bare SiNW. Simultaneously, when the light was turned off, the current density showed a shift in the direction opposite to J_{in}, which was designated as J_{off}. The J_{off} values of the rGO-SiNW and SiNW electrodes were 0.18 mA/cm^2 and -0.16 mA/cm^2, respectively. The small J_{off} of the rGO-SiNW electrode suggest that less charge carriers were trapped and recombination rate was much smaller at the surface of electrode when compared to those of the SiNW sample.

Capacitance measurements also showed that rGO catalyst is much more effective for the electrochemical hydrogen production. Potential sweep ranging from 0.4 V to -0.3 V vs. RHE under dark condition as shown in Figure 5b and the flat band potential was calculated using the Mott-Schottky equation:[23]

$$1/C_{sc}^2=2(E-E_{fb}-kT/e)/(e\varepsilon\varepsilon_0 N) \quad (4)$$

where C_{sc} is the capacitance in space charge region, E is the applied potential, and the E_{fb} is the flat band potential which can be determined from the extrapolation to the capacitance of zero (Figure 5b), k is the Planck constant, T is the temperature, e is the electron charge, ε is the dielectric constant of the Si semiconductor (photoelectrode), ε_0 is the permittivity of the free space, N is the hole acceptor concentration for the p-type Si semiconductor, which is calculated from the slope in the figure plot shown above. On the basis of these relations, rGO-SiNW exhibits an E_{fb} of 0.128 V vs. RHE, which is 88 mV higher than the E_{fb} for the bare SiNW. The higher E_{fb} indicates the band bending near the depletion the semiconductor near at the electrode/electrolyte interface is higher, based on this equation the magnitude of the band bending (E_b) is equals to $E - E_{fb}$.[24] The band bending at the boundary between

Peer-reviewed version available at Appl. Sci. 2018, 8, 2046; doi:10.3390/app8112046

the electrode surface and electrolyte accelerates for a fast separation of charge carriers and increase in recombination of protons to generate hydrogen.[25] To conclude, the capacitance and transient photoresponse measurements from the results substantiate that rGO-SiNW system is highly active in terms of decrease in recombination of charge carriers and reduces the energy barrier for HER along the electrode/electrolyte interface.

5. Conclusions

In conclusion, we fabricated reduced graphene oxide (rGO) co-catalyst on the silicon nanowire (SiNW) photocathode system. The surface nanostructuring of the SiNW photocathode showed the enhanced property for the hydrogen evolution reaction (HER). Moreover, deposition of rGO co-catalyst onto the SiNW showed even 158 times higher conversion efficiency than bare planar Si without any co-catalyst and also indicated 3.47 times higher efficiency than bare SiNW, respectively. As a result, rGO displayed a remarkable catalytic activity meant for the photoeletrochemical HER on SiNW photocathodes. We believe that the optimization of interface engineering between the co-catalyst and the photoelectrode in this study would pave way for realizing metal-free carbon-based catalysts with high efficacy for effectual solar-driven hydrogen fuel production.

Author Contributions: Conceptualization, U.S. and J.M.; Methodology, U.S.; Validation, U.S. and J.M.; Formal Analysis, Y.S.; Investigation, U.S.; Resources, U.S.; Data Curation, U.S.; Writing-Original Draft Preparation, Y.S. and J. J.; Writing-Review & Editing, J. J., U.S., and J.M.; Visualization, Y.S.; Supervision and Project Administration, J. M. and U.S. ǂ and * These authors contributed equally to this work.

Acknowledgments: This research was supported by the Basic Science Research Program through the National Research Foundation of Korea funded by the Ministry of Science and ICT (NRF-2017M3A7B4049176, 2018R1C1B6001267, and 2018R1A5A1025224).

Conflicts of Interest: The authors declare no conflict of interest.

References

1. Chu, S.; Cui, Y.; Liu, N., The path towards sustainable energy. *Nature Materials* **2016,** *16*, 16.
2. Turner, J. A., Sustainable Hydrogen Production. *Science* **2004,** *305* (5686), 972-974.
3. Popczun, E. J.; McKone, J. R.; Read, C. G.; Biacchi, A. J.; Wiltrout, A. M.; Lewis, N. S.; Schaak, R. E., Nanostructured Nickel Phosphide as an Electrocatalyst for the Hydrogen Evolution Reaction. *Journal of the American Chemical Society* **2013,** *135* (25), 9267-9270.
4. Ni, M.; Leung, M. K. H.; Leung, D. Y. C.; Sumathy, K., A review and recent developments in photocatalytic water-splitting using TiO2 for hydrogen production. *Renewable and Sustainable Energy Reviews* **2007,** *11* (3), 401-425.
5. Cook, T. R.; Dogutan, D. K.; Reece, S. Y.; Surendranath, Y.; Teets, T. S.; Nocera, D. G., Solar Energy Supply and Storage for the Legacy and Nonlegacy Worlds. *Chemical Reviews* **2010,** *110* (11), 6474-6502.
6. Warren, S. C.; Voïtchovsky, K.; Dotan, H.; Leroy, C. M.; Cornuz, M.; Stellacci, F.; Hébert, C.; Rothschild, A.; Grätzel, M., Identifying champion nanostructures for solar water-splitting. *Nature materials* **2013,** *12* (9), 842.
7. Wang, X.; Peng, K. Q.; Pan, X. J.; Chen, X.; Yang, Y.; Li, L.; Meng, X. M.; Zhang, W. J.; Lee, S. T., High-Performance Silicon Nanowire Array Photoelectrochemical Solar Cells

Peer-reviewed version available at *Appl. Sci.* **2018**, *8*, 2046; doi:10.3390/app8112046

through Surface Passivation and Modification. *Angewandte Chemie International Edition* **2011,** *50* (42), 9861-9865.

8. Oh, I.; Kye, J.; Hwang, S., Enhanced Photoelectrochemical Hydrogen Production from Silicon Nanowire Array Photocathode. *Nano Letters* **2011,** *12* (1), 298-302.

9. Oh, I.; Kye, J.; Hwang, S., Enhanced Photoelectrochemical Hydrogen Production from Silicon Nanowire Array Photocathode. *Nano Letters* **2012,** *12* (1), 298-302.

10. Hou, Y.; Abrams, B. L.; Vesborg, P. C. K.; Björketun, M. E.; Herbst, K.; Bech, L.; Setti, A. M.; Damsgaard, C. D.; Pedersen, T.; Hansen, O.; Rossmeisl, J.; Dahl, S.; Nørskov, J. K.; Chorkendorff, I., Bioinspired molecular co-catalysts bonded to a silicon photocathode for solar hydrogen evolution. *Nat Mater* **2011,** *10* (6), 434-438.

11. Warren, E. L.; McKone, J. R.; Atwater, H. A.; Gray, H. B.; Lewis, N. S., Hydrogen-evolution characteristics of Ni–Mo-coated, radial junction, n+p-silicon microwire array photocathodes. *Energy & Environmental Science* **2012,** *5* (11), 9653-9661.

12. Seger, B.; Laursen, A. B.; Vesborg, P. C. K.; Pedersen, T.; Hansen, O.; Dahl, S.; Chorkendorff, I., Hydrogen Production Using a Molybdenum Sulfide Catalyst on a Titanium-Protected n+p-Silicon Photocathode. *Angewandte Chemie International Edition* **2012,** *51* (36), 9128-9131.

13. Huang, Z.; Zhong, P.; Wang, C.; Zhang, X.; Zhang, C., Silicon nanowires/reduced graphene oxide composites for enhanced photoelectrochemical properties. *ACS Appl Mater Interfaces* **2013,** *5* (6), 1961-6.

14. Meng, H.; Fan, K.; Low, J.; Yu, J., Electrochemically reduced graphene oxide on silicon nanowire arrays for enhanced photoelectrochemical hydrogen evolution. *Dalton Trans* **2016,** *45* (35), 13717-25.

15. Hu, L.; Chen, G., Analysis of Optical Absorption in Silicon Nanowire Arrays for Photovoltaic Applications. *Nano Letters* **2007,** *7* (11), 3249-3252.

16. Sim, U.; Moon, J.; An, J.; Kang, J. H.; Jerng, S. E.; Moon, J.; Cho, S.-P.; Hong, B. H.; Nam, K. T., N-doped graphene quantum sheets on silicon nanowire photocathodes for hydrogen production. *Energy & Environmental Science* **2015,** *8* (4), 1329-1338.

17. Garnett, E.; Yang, P., Light Trapping in Silicon Nanowire Solar Cells. *Nano Letters* **2010,** *10* (3), 1082-1087.

18. Tian, B.; Zheng, X.; Kempa, T. J.; Fang, Y.; Yu, N.; Yu, G.; Huang, J.; Lieber, C. M., Coaxial silicon nanowires as solar cells and nanoelectronic power sources. *Nature* **2007,** *449*, 885.

19. Zhu, J.; Yu, Z.; Burkhard, G. F.; Hsu, C.-M.; Connor, S. T.; Xu, Y.; Wang, Q.; McGehee, M.; Fan, S.; Cui, Y., Optical Absorption Enhancement in Amorphous Silicon Nanowire and Nanocone Arrays. *Nano Letters* **2009,** *9* (1), 279-282.

20. Chen, J.; Yao, B.; Li, C.; Shi, G., An improved Hummers method for eco-friendly synthesis of graphene oxide. *Carbon* **2013,** *64*, 225-229.

21. Oh, J.; Deutsch, T. G.; Yuan, H.-C.; Branz, H. M., Nanoporous black silicon photocathode for H2 production by photoelectrochemical water splitting. *Energy & Environmental Science* **2011,** *4* (5), 1690-1694.

22. Allen J. Bard, L. R. F., Electrochemical Methods: Fundamentals and Applications. *John Wiley & Sons, Inc.* **2001**, 864.

23. Bott, A. W., Electrochemistry of Semiconductors. *Current Separations* **1998,** *17* (3), 87-91.

24. Gelderman, K.; Lee, L.; Donne, S. W., Flat-Band Potential of a Semiconductor: Using the Mott–Schottky Equation. *Journal of Chemical Education* **2007,** *84* (4), 685.

Peer-reviewed version available at *Appl. Sci.* **2018**, *8*, 2046; doi:10.3390/app8112046

25. Lewis, N. S., A Quantitative Investigation of the Open-Circuit Photovoltage at the Semiconductor/Liquid Interface. *Journal of The Electrochemical Society* **1984,** *131* (11), 2496-2503.